A Possible Mechanism of Stabilization of Emulsions by Solid Particles

Possible explanations of some experimental findings with emulsions stabilized by small adsorbed solid particles are proposed. Films consisting of a particle monolayer are considered and the stability of the liquid menisci between the particles is investigated theoretically. The effect of contact angle hysteresis on the effective disjoining pressure isotherms is also taken into account.

1. INTRODUCTION

Pickering (1) showed that finely divided powders can be very efficient emulsion-stabilizing agents, and the main factors affecting the stability were summarized by Tadros and Vincent (2) as follows:

(i) The particles have to be very finely divided;
(ii) The contact angle formed between the liquid–liquid interface and the particle surface must be close to 90° (higher or lower depending on the type of the emulsion); and
(iii) The rougher the particles (i.e., the higher the hysteresis of the contact angle), the higher the stabilizing efficiency.

Tadros and Vincent argued (correctly) that "Presumably, the presence of solid particles . . . plays an important role in preventing the thinning of the liquid film between the droplets" (see Fig. 1a). They also presented a simplified theory of the energy of adsorption of solid particles at a liquid–liquid interface. A more refined theory of the energy of adsorption was developed by Levine *et al.* (3). The energy of adsorption is certainly an important factor in determining the stabilizing efficiency because the adsorbed layer must be dense enough for stabilization to occur. Yet, it cannot be the factor "preventing the thinning of the liquid film" (see above). In this paper we show that the capillary pressure arising from the deformation of the liquid interface around the adsorbed particles when the liquid is squeezed out of the thin film could be such a factor.

2. STABILITY OF THIN FILMS TO RUPTURE

As known, the emulsions are stable when the thin film formed between two colliding drops is sufficiently stable to resist rupture. Fig. 1a represents a model of such a film stabilized by uniformly distributed microscopic spherical solid particles of equal size. The type of the discontinuous phase 2 (oil or water) does not affect the analysis developed below. The pressure inside and outside the attached drops will be denoted by P_1 and P_2, respectively. Then the capillary pressure of the droplets is

$$P_c = P_1 - P_2. \qquad [2.1]$$

A reason for the existence of such a difference between P_1 and P_2 can be either curvature of the drop surface or gravitational (hydrostatic) sucking pressure in an emulsion column.

When $P_c = 0$, the particles and the surrounding menisci will be situated as depicted in Fig. 1b (negligible gravity). However, when $P_c \neq 0$ the liquid interface around each particle will deform (see Fig. 1c). For rupture of the film to occur, it is necessary for the shortest distance between the two film surfaces (denoted by h in Fig. 1) to become zero. More precisely, the rupture takes place at some small nonzero critical thickness (see, e.g., (4)) that is neglected here.

To estimate the capillary pressure necessary to rupture the film, we will consider the liquid meniscus around a particle to be approximately axisymmetric. More precisely, in our model each adsorbed particle occupies a circular cell of area A_0, which is equal to the mean area per particle in the real film. The meniscus profile obeys the Laplace equation (5),

$$\frac{1}{r}\frac{d}{dr}(r \sin \phi) = P_c/\gamma_{12} \qquad [2.2]$$

$$\frac{dz}{dr} = \tan \phi. \qquad [2.3]$$

Here γ_{12} is interfacial tension of the liquid–liquid interface, $z = z(r)$ is the generatrix of the meniscus profile, and $\phi = \phi(r)$ is the running slope angle (Fig. 1c). We suppose that at the boundary of each cell,

$$\phi(b) = 0, \qquad [2.4]$$

where b is the radius of the cell ($\pi b^2 = A_0$). The relation between the value of b and the distance between particles in the film depends on their arrangement. Anyhow, the value of b/a cannot be less than $\sqrt{(2\sqrt{3})/\pi}$, which corresponds to hexagonal close-packing of the particles.

The integration of Eq. [2.2] along with the boundary condition [2.4] yields

$$\sin \phi = p(b^2 - r^2)/ar, \qquad [2.5]$$

where

$$p = P_c a/(2\gamma_{12}) \qquad [2.6]$$

0021-9797/92 $3.00

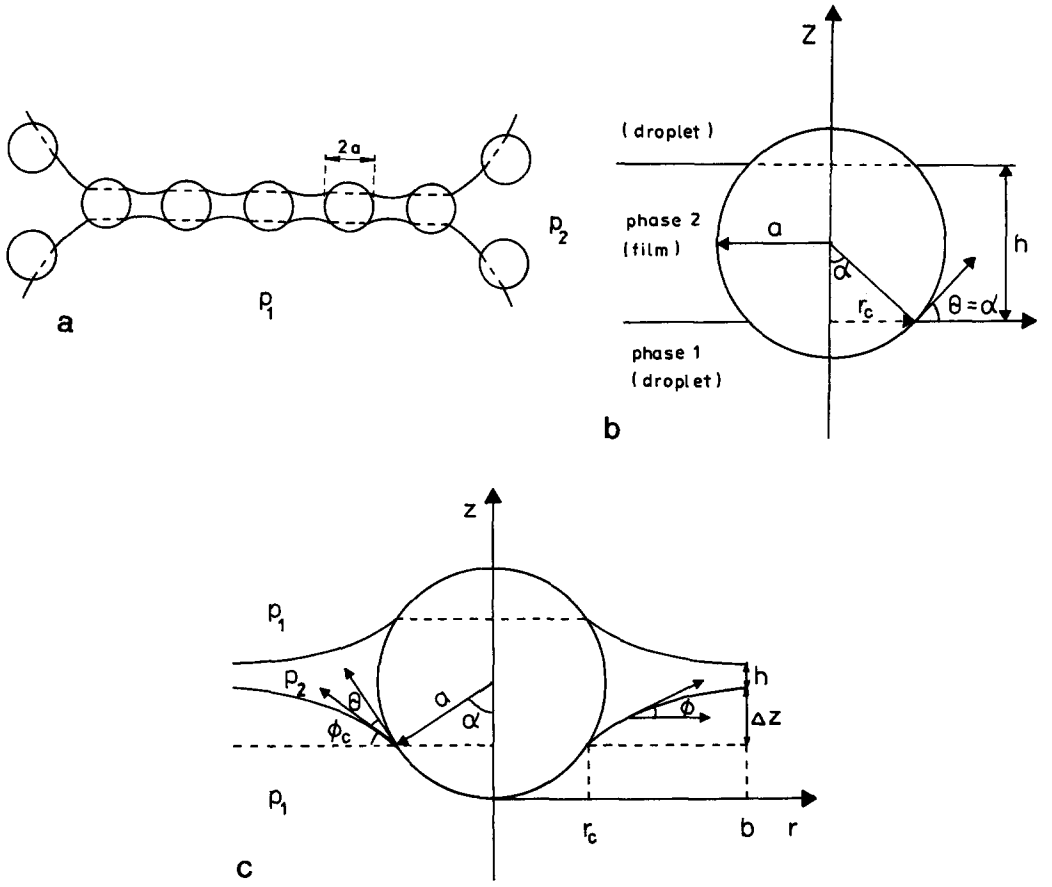

FIG. 1. Sketch of a film formed between two emulsion drops stabilized by spherical solid particles (a); $P_c = P_1 - P_2$ is the capillary pressure; the cases with $P_c = 0$ and $P_c > 0$ are depicted in (b) and (c), respectively.

is the dimensionless capillary pressure. By integrating Eq. [2.3], along with Eq. [2.5], one can determine the elevation,

$$\Delta z = \int_{r_c}^{b} \frac{(b^2 - r^2)dr}{[(ar/p)^2 - (b^2 - r^2)^2]^{1/2}}, \qquad [2.7]$$

of the meniscus above the level of the contact line (see Fig. 1c). The smallest thickness of the film will be

$$h = 2(a \cos \alpha - \Delta z) \qquad [2.8]$$

(see Fig. 1c for notation).

Below we will investigate the dependence $p = p(h)$ in the following two cases: (i) movement of the contact line at constant contact angle θ and (ii) changing contact angle θ at immobile contact line. The dependence of $p(h)$ on the size of the cells b will be also considered.

a. Movement of the Contact Line at Constant Contact Angle

This case can be realized (i) when there is no hysteresis of the contact angle and its equilibrium value $\theta = \theta_e$ is preserved during the motion of the contact line, and (ii) when during the receding of the meniscus the contact angle acquires some dynamic value $\theta = \theta_r = \text{const}$.

Simple geometrical considerations (Fig. 1c) yield

$$r_c = a \sin \alpha = a \sin(\phi_c + \theta). \qquad [2.9]$$

In addition, by setting $r = r_c$ in Eq. [2.5] one obtains

$$p = \frac{ar_c \sin \phi_c}{b^2 - r_c^2}. \qquad [2.10]$$

Equations [2.7–2.10] enable one to calculate the dependence $p(h)$ for given values of the contact angle θ and

radius of the cell b. Such curves are presented as the solid lines in Fig. 2 for $b = 1.5a$ and $\theta = 0$, 30, 60, and 75°.

One sees that h decreases with increasing P_c. Let p^* be the value of the (dimensionless) capillary pressure at which $h = 0$ (points M_1–M_4 in Fig. 2). p^* represents the maximum value of the (dimensionless) capillary pressure that can be resisted by the liquid meniscus at given θ and b. In other words, p^* is the threshold of film rupture. It turns out that p^* is largest at $\theta = 0°$ (point M_1 in Fig. 2) and equals zero at $\theta = 90°$. Films with configuration like that shown in Fig. 1 are not compatible with $\theta > 90°$.

b. Contact Angle Hysteresis

Usually the particle surface is rough or inhomogeneous and large contact angle hysteresis can be observed experimentally (2). Let us imagine a process of pressing the film surfaces (Fig. 1) by increasing the capillary pressure. In the beginning the contact angle will decrease from $\theta = \theta_e$ to $\theta = \theta_r$ at fixed contact radius r_c (see Fig. 1c). Then the meniscus will start to recede (i.e., r_c changes) with constant dynamic contact angle $\theta = \theta_r$. The difference,

$$\theta_h = \theta_e - \theta_r, \qquad [2.11]$$

characterizes the contact angle hysteresis.

Let us first consider the change of θ from θ_e to θ_r at r_c = const. In view of Eq. [2.9], α will be also constant: $\alpha = \theta_e$. ϕ_c will change from zero up to $\phi_{cr} = \alpha - \theta_r = \theta_h$. According to Eqs. [2.9] and [2.10] the (dimensionless) capillary pressure will change from zero up to a value

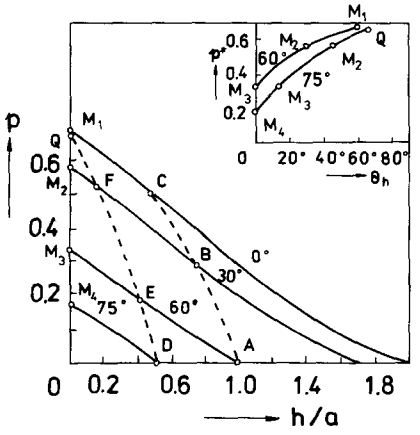

FIG. 2. Plot of the dimensionless capillary pressure p vs the dimensionless thickness of the liquid meniscus, h/a; the full and the broken lines correspond to fixed contact angle θ and contact radius r_c, respectively. The inset represents the dimensionless maximum meniscus pressure, p^*, vs the contact angle hysteresis, θ_h.

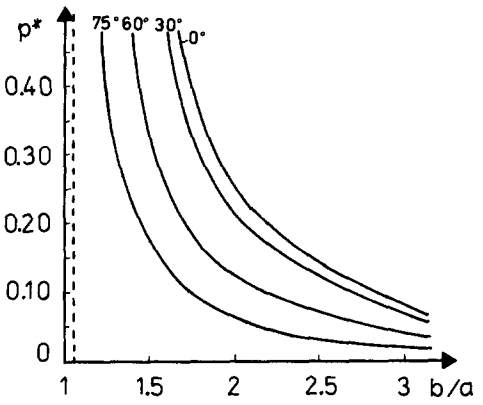

FIG. 3. Plot of the dimensionless maximum meniscus pressure, p^*, vs the dimensionless radius of the unit cell, b/a. The vertical dashed line corresponds to $b/a = 1.050$ (hexagonal close-packing of the particles).

$$p_r = \frac{\sin\theta_e \sin\theta_h}{\lambda^2 - \sin^2\theta_e}, \qquad [2.12]$$

where $\lambda = b/a$. Eqs. [2.7–2.8] yield the respective values of h.

Each of the broken lines in Fig. 2 represents the dependence of p on h during a process of decreasing θ at r_c = const. Point A in Fig. 2 corresponds to an initial state with $\theta = \theta_e = 60°$ and $p = 0$ (see Fig. 1b). When decreasing θ the capillary pressure changes along the curve AB. If the hysteresis is $\theta_h = 30°$ ($\theta_r = 30°$), point B represents the onset of the meniscus's receding. In such a case a further increase of the capillary pressure will follow the curve BM_2 and the film will rupture at the point M_2.

If the hysteresis is $\theta_h = 60°$ ($\theta_r = 0°$), the increasing capillary pressure will first follow curve AC and then curve CM_1. In this case points C and M_1 correspond to the onset of the receding and to the film rupture, respectively.

Point D in Fig. 2 corresponds to another initial state with $\theta = \theta_e = 75°$C and $p = 0$. In this case when θ decreases, the capillary pressure p increases along curve DF. If the hysteresis is $\theta_h = 45°$ ($\theta_r = 30°$), $p(h)$ will follow the curves DF and FM_2. It turns out that in this case ($\theta_e = 75°$), hysteresis θ_h greater than 66.5° (point Q in Fig. 2 where $h = 0$) cannot be observed.

From this consideration one sees that when contact angle hysteresis occurs, the threshold of film rupture depends on θ_h. This dependence is illustrated in the inset of Fig. 2 for two equilibrium contact angles, $\theta_e = 60$ and 75°. One sees that in both cases the maximum capillary pressure p^* increases with increasing contact angle hysteresis and hence, the film stability also increases. In addition, the dimensional maximum capillary pressure is $P_c^{max} = (2\gamma_{12}p^*)/a$ (Eq. [2.6]), and therefore P_c^{max} and the film stability will increase with decreasing particle radius a.

The latter two conclusions correlate well with the experimental findings (see the beginning of this paper).

c. *Dependence of the Threshold of Film Rupture on the Distance between the Adsorbed Particles*

For particle radius $a = 1\ \mu m$ and $\gamma_{12} = 30\ mN/m$, P_c^{max} varies between 1×10^4 and $4.2 \times 10^4\ Pa$ for the curves shown in the inset of Fig. 2. These thresholds seem to be too high to be easily overcome. This fact correlates with the high stability of emulsion films, whose surfaces are covered by solid particles. A rupture of the film is possible only if the distance, d, between the particles is large enough. If we assume a hexagonal packing, then $d = b\sqrt{(8\sqrt{3})/\pi}$ with b being the radius of an elementary cell in our model.

The dependence of p^* on the dimensionless radius of the cell, $\lambda = b/a$, is shown in Fig. 3. As noted above, the value of λ cannot be less than 1.050 (the vertical dashed line in Fig. 3), the latter value corresponding to hexagonal close-packing of the particles. One sees that p^* steeply increases with the decrease of λ. For example, with $\theta = 60°$, $a = 1\ \mu m$, and $\gamma_{12} = 30\ mN/m$, one calculates $P_c^{max} = 2.7 \times 10^5\ Pa$ for $b = 1.050a$, $P_c^{max} = 7.8 \times 10^3\ Pa$ for $b = 2a$, and $P_c^{max} = 2.4 \times 10^3\ Pa$ for $b = 3a$. The numerical calculations show that for dense monolayers ($\lambda \approx 1$) the threshold of film rupture is very high ($P_c^{max} \sim 10^5\ Pa$) and cannot be easily overcome. So the corresponding films are to be stable. At larger interparticle distances the threshold of film rupture can be orders of magnitude lower.

3. ROLE OF THE ADSORPTION ENERGY

The results presented in Figs. 2 and 3 demonstrate that the lower the contact angle, the higher the threshold of rupture. On the other hand, the contact angle is a factor governing the stable position of an adsorbed particle at the emulsion interface.

The surface free energy of a particle attached to an interface is (2)

$$G = \gamma_{1s}A_{1s} + \gamma_{2s}A_{2s} + \gamma_{12}A_{12}, \qquad [3.1]$$

where A is surface area, γ is surface free energy per unit area, the subscript "s" denotes the solid particle, and the subscripts 1 and 2 denote the two immiscible liquid phases. To estimate G we will consider a spherical particle adsorbed at a planar interface (negligible gravity and other external forces). Simple geometrical considerations yield

$$G = W(\theta) + \text{const}, \qquad [3.2]$$

where

$$W(\theta) = 2\pi a^2[\gamma_{1s}(1 - \cos\theta) + \gamma_{2s}(1 + \cos\theta) - \tfrac{1}{2}\gamma_{12}\sin^2\theta]. \qquad [3.3]$$

W vs θ is a curve having a minimum at $\theta = \theta_e$, where θ_e is defined through the Young equation

$$\gamma_{12}\cos\theta_e = \gamma_{1s} - \gamma_{2s}, \qquad [3.4]$$

i.e., θ_e is the equilibrium value of the contact angle. The values $\theta = \pi$ and $\theta = 0$ correspond to a particle which is entirely situated in phase 1 or 2, respectively. Hence

$$\Delta W_1 = W(\pi) - W(\theta_e),$$
$$\Delta W_2 = W(0) - W(\theta_e) \qquad [3.5]$$

are the barriers preventing the particle's detachment from the emulsion interface. By using Eqs. [3.3] and [3.4] one derives (2)

$$\Delta W_1 = \pi a^2\gamma_{12}(1 - \cos\theta_e)^2,$$
$$\Delta W_2 = \pi a^2\gamma_{12}(1 + \cos\theta_e)^2. \qquad [3.6]$$

Eq. [3.6] shows that if θ_e is less than 90°, ΔW_1 will be smaller than and ΔW_2 will be greater than $\pi a^2\gamma_{12}$; hence the detachment of the particle toward phase 1 will be enhanced. Analogously, if θ_e is greater than 90°, then ΔW_2 will be less than $\pi a^2\gamma_{12}$ and the particle's detachment toward phase 2 will be enhanced. In other words, when $\theta_e \neq 90°$, one of the two barriers is less than $\pi a^2\gamma_{12}$. For $\theta_e = 90°$ both barriers are equal to $\pi a^2\gamma_{12}$, and obviously this is the most stable position of the particle at the interface.

Now let us imagine two approaching emulsion droplets covered by a layer of small solid particles. The hydrodynamic friction forces accompanying the drainage of the film formed between the two colliding drops (see, e.g., (7)) will disturb the particles and will enable them to overcome the lower of the two barriers (ΔW_1 or ΔW_2). Depending on the value of θ_e a detached particle can be enhanced to enter the continuous or the discontinuous emulsion phase. However, in both cases the result is the same: decreased surface density of the adsorbed solid particles and decreased emulsion stability. The hydrodynamic detachment of particles should be even more pronounced when there is stirring of the emulsion or vertical droplet motion due to gravity. In this aspect, an equilibrium contact angle close to 90° is the most favorable for the emulsion stability.

In summary, from adsorption energy considerations it follows that the particle attachment is most stable at $\theta_e = 90°$ and most unstable at $\theta_e = 0°$. Just the opposite, the liquid menisci are most stable at $\theta_e = 0°$ and most unstable at $\theta_e = 90°$ (see above). The combination of these two effects, energy of particle detachment and threshold of film rupture, leads to the conclusion that θ_e should not be too close to 0 or 90° for the most stable films. The experimental finding (ii) cited in the Introduction of this note suggests that the hydrodynamic interactions can play an important role in determining the emulsion stability.

4. DISJOINING PRESSURE DUE TO ADSORBED PARTICLES

The integral capillary force exerted on an adsorbed particle from one of the film surfaces (Fig. 1) is

$$F = 2\pi r_c \gamma_{12} \sin \phi_c + \pi r_c^2 P_c. \quad [4.1]$$

The first term on the right-hand side of Eq. [4.1] accounts for the contribution of the meniscus surface tension, whereas the second term is due to the pressure drop across the film surface. Let us introduce the quantity

$$\Pi^p = F/(\pi b^2) = 2\gamma_{12} \frac{r_c}{b^2} \sin \phi_c + \frac{r_c^2}{b^2} P_c, \quad [4.2]$$

where πb^2 is the area per adsorbed particle. Π^p can be interpreted as a disjoining pressure due to the adsorbed particles. Indeed, at equilibrium ϕ_c obeys Eq. [2.10]. Then substitution from Eqs. [2.6] and [2.10] into Eq. [4.2] yields

$$\Pi^p = P_c, \quad [4.3]$$

which is the well-known condition for equilibrium (see, e.g., (6)). Hence the $p(h)$ curves in Fig. 3 in fact represent equilibrium disjoining pressure isotherms. (It should be noted that the quantity h, as defined in the present study, does not coincide with the thermodynamic film thickness that is currently used in the thermodynamics of thin liquid films without particles (see, e.g., (6)).

5. CONCLUSIONS

In this study we propose possible explanations of some experimental findings with emulsions stabilized by small adsorbed solid particles. Namely, experiments show that the emulsion stability is increased (i) when the contact angle is less than 90° but close to 90°, (ii) when its hysteresis is larger, and (iii) when the particles are smaller.

It turns out that the "activation energy" needed for particle desorption from the emulsion interface is the largest when the contact angle equals 90°. In addition, we considered theoretically films formed by a particle monolayer pressed between two emulsion interfaces (Fig. 1). Their stability is determined by the maximum capillary pressure drop, P_c^{max}, which can be resisted by liquid menisci formed between the adsorbed particles. It turns out that P_c^{max} is greater when the hysteresis is larger and when the particles are smaller. These findings are in consonance with the experimental results. Besides, an effective disjoining pressure due to the adsorbed particles can be introduced. The theoretical analysis performed is equally applicable to both oil-in-water and water-in-oil emulsions. The predictions of the theoretical model developed in the present paper are subject to direct verification in experiments with emulsion films.

In the model under consideration uniform distribution of particles in the film is supposed. From a physical viewpoint this will be the case when repulsion between the particles in the film takes place. In the opposite case, when there is attraction between the particles, they can aggregate and the film will rupture at lower pressure due to the "holes" or "cracks" formed. We do not consider such a possibility here because the problem of the interaction between solid particles via surrounding menisci has not yet been solved for such a complicated configuration. In the present study we also do not report the results for films formed by two attached monolayers of adsorbed solid particles. Such a configuration is possible only if the distance between the adsorbed particles is close to the minimum. Our calculations showed that in this case the threshold of film rupture is extremely high and the films are very stable.

REFERENCES

1. Pickering, S. U., *J. Chem. Soc.* **91,** 2001 (1907).
2. Tadros, Th. V., and Vincent, B., "Encyclopedia of Emulsion Technology" (P. Becher, Ed.), Vol. 1, p. 129. Dekker, New York, 1983.
3. Levine, S., Bowen, B. D., and Partridge, S. J., *Colloids Surf.* **38,** 325 and 345 (1989).
4. Hartland, S., *in* "Thin Liquid Films" (I. B. Ivanov, Ed.), p. 663. Dekker, New York, 1988.
5. Princen, H. M., *in* "Surface and Colloid Science" (E. Matijevic, Ed.), Vol. 2, p. 1. Wiley-Interscience, New York, 1969.
6. de Feijter, J. A., *in* "Thin Liquid Films" (I. B. Ivanov, Ed.), p. 1. Dekker, New York, 1988.
7. Ivanov, I. B., and Dimitrov, D. S., *in* "Thin Liquid Films" (I. B. Ivanov, Ed.), p. 379. Dekker, New York, 1988.

N. D. DENKOV
I. B. IVANOV [1]
P. A. KRALCHEVSKY

Laboratory of Thermodynamics and Physico-Chemical Hydrodynamics
University of Sofia, Faculty of Chemistry
Sofia 1126, Bulgaria

D. T. WASAN

Department of Chemical Engineering
Illinois Institute of Technology
Chicago, Illinois 60616

Received April 15, 1991; accepted September 19, 1991

[1] To whom correspondence should be addressed.